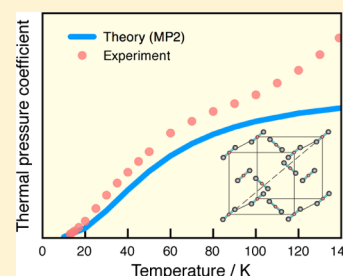


# Second-Order Many-Body Perturbation Study on Thermal Expansion of Solid Carbon Dioxide

Jinjin Li,<sup>†</sup> Olaseni Sode,<sup>‡</sup> and So Hirata<sup>\*,†,§</sup><sup>†</sup>Department of Chemistry, University of Illinois at Urbana-Champaign, 600 South Mathews Avenue, Urbana, Illinois 61801, United States<sup>‡</sup>Department of Chemistry, University of Chicago, 5735 South Ellis Avenue, Chicago, Illinois 60637, United States<sup>§</sup>CREST, Japan Science and Technology Agency, 4-1-8 Honcho, Kawaguchi, Saitama 332-0012, Japan

**ABSTRACT:** An embedded-fragment *ab initio* second-order many-body perturbation (MP2) method is applied to an infinite three-dimensional crystal of carbon dioxide phase I (CO<sub>2</sub>-I), using the aug-cc-pVDZ and aug-cc-pVTZ basis sets, the latter in conjunction with a counterpoise correction for the basis-set superposition error. The equation of state, phonon frequencies, bulk modulus, heat capacity, Grüneisen parameter (including mode Grüneisen parameters for acoustic modes), thermal expansion coefficient ( $\alpha$ ), and thermal pressure coefficient ( $\beta$ ) are computed. Of the factors that enter the expression of  $\alpha$ , MP2 reproduces the experimental values of the heat capacity, Grüneisen parameter, and molar volume accurately. However, it proves to be exceedingly difficult to determine the remaining factor, the bulk modulus ( $B_0$ ), the computed value of which deviates from the observed value by 50–100%. As a result,  $\alpha$  calculated by MP2 is systematically too low, while having the correct temperature dependence. The thermal pressure coefficient,  $\beta = \alpha B_0$ , which is independent of  $B_0$ , is more accurately reproduced by theory up to 100 K.



## 1. INTRODUCTION

Thermal expansion<sup>1</sup> of materials is a major concern in manufacturing, construction, and precision engineering. That of molecular crystals of atmospheric species, such as ice on the Earth and dry ice on other planetary bodies, can have a significant effect on their climate. Some of these molecular crystals exist in extreme conditions (e.g., high pressures and low temperatures) and can be difficult to probe experimentally.<sup>2</sup> It is thus of interest to establish a computational method that can predict the coefficients of thermal expansion of solids from first principles.

Solid carbon dioxide phase I (CO<sub>2</sub>-I) or dry ice has a large thermal expansion coefficient for a solid.<sup>3</sup> This is clearly related to its large heat capacity and low sublimation temperature. Maass and Barnes<sup>3</sup> were the first to report its thermal expansion coefficient ( $\alpha$ ) at intermediate temperatures ( $T$ ). Their values were, however, systematically overestimated according to a later, more comprehensive study by Manzhelii et al.,<sup>4</sup> who also measured  $\alpha$  at low temperatures, molar isobaric heat capacity ( $C_p$ ), and velocities of ultrasonic waves. With these, they calculated the values of molar isochoric heat capacity ( $C_v$ ), Grüneisen parameter ( $\gamma$ ), and compressibility. The values of  $\alpha$  in a wider temperature range were reported by Krupskii et al.,<sup>5</sup> which were in accurate agreement with those of Manzhelii et al.<sup>4</sup> All previous computational studies<sup>6–10</sup> on thermal expansion of CO<sub>2</sub>-I were based on empirical intermolecular potentials.

Giordano et al.<sup>11</sup> reported a Mie–Grüneisen–Debye equation of state of CO<sub>2</sub>-I over its entire range of stability. It was obtained by fitting to a large body of then-existing and new thermodynamic and spectroscopic data (see, e.g., Jäger and

Span<sup>12</sup> for the latest compilation). Using this equation of state, they were able to reproduce quantitatively the measured values of  $\alpha$  in a wide range of temperatures. This agreement was, however, possible with the assumption that the Grüneisen parameter ( $\gamma$ ) was twice as large as the experimentally measurable mode Grüneisen parameters ( $\gamma_{ik}$ ) of zone-center phonons. The former was also assumed to increase linearly with volume. The authors concluded: “To go further, it is necessary to determine the full spectrum of phonons, which should be accessible either through the use of inelastic x-ray or neutron scattering techniques, or through calculations.”<sup>11</sup> A more recent, related work by Trusler,<sup>13,14</sup> which was based on an even larger data set, found a much smaller fitted value of  $\gamma$ , which was also to decrease slightly with volume, instead of increase.

Here, we report a first-principles calculation of  $\gamma_{ik}$  for optical as well as acoustic modes not just at the zone center but throughout the Brillouin zone of an infinite three-dimensional crystal of CO<sub>2</sub>-I. We then compute  $\gamma$ ,  $C_v$ , bulk modulus at zero pressure ( $B_0$ ), and finally  $\alpha$  in the temperature range 0–200 K. The calculation is based on the embedded-fragment *ab initio* second-order many-body perturbation (MP2) method<sup>15,16</sup> with and without a counterpoise correction for the basis-set superposition error (BSSE) and involves no adjustable parameter fitted to experimental data. Two basis sets (aug-cc-pVDZ and aug-cc-pVTZ) are used.

We show that the MP2-calculated values of  $\gamma$  are nearly constant at 2.0 and are in excellent agreement with the

Received: September 18, 2014

Published: December 9, 2014

experimental values of Manzhelii et al.,<sup>4</sup> until the latter begin to increase at  $T \approx 100$  K. They are closer to the values and temperature dependence of  $\gamma$  assumed by Trusler<sup>13,14</sup> than those of Giordano et al.<sup>11</sup> and support Manzhelii's interpretation of the increase at  $T \approx 100$  K in terms of defects.<sup>4</sup> Nevertheless, the MP2-predicted value of  $\alpha$  is significantly underestimated, while reproducing its temperature dependence well up to 100 K. This is traced, nearly entirely, to large errors (50–100%) in the calculated values of  $B_0$ ,  $C_V$ ,  $\gamma$ , the molar volume at zero pressure ( $V_0$ ), and the individual values of  $\gamma_{ik}$  are all reproduced reasonably accurately by MP2. The thermal pressure coefficient ( $\beta$ ),<sup>17,18</sup> whose evaluation does not involve  $B_0$  and which should be directly measurable, agrees well between theory and experiments.

## 2. COMPUTATIONAL METHOD

Thermal expansion is an anharmonic effect.<sup>19</sup> In the quasiharmonic approximation, this effect is accounted for by considering the variation of harmonic frequencies with volume according to Grüneisen's theory.<sup>1</sup> The volumetric and linear thermal expansion coefficients, denoted respectively by  $\alpha_V$  and  $\alpha_L$ , are then given by

$$\alpha_V = 3\alpha_L = \frac{C_V \gamma}{V_0 B_0} \quad (1)$$

where the Grüneisen parameter ( $\gamma$ ) is written as

$$\gamma = \frac{1}{\tilde{C}_V K} \sum_i \sum_{\mathbf{k}} \gamma_{ik} c_{ik} \quad (2)$$

Here,  $ik$  labels the phonon on the  $i$ th dispersion branch with wave vector  $\mathbf{k}$  and  $\tilde{C}_V$  is the "unit-cell" isochoric heat capacity to be defined below. There are  $K$  evenly spaced  $\mathbf{k}$  points in the reciprocal unit cell.

The mode Grüneisen parameter ( $\gamma_{ik}$ ) and mode heat capacity ( $c_{ik}$ ) (both unitless) are calculated as

$$\gamma_{ik} = -\frac{V}{\omega_{ik}} \frac{\partial \omega_{ik}}{\partial V} = -\frac{\partial \ln \omega_{ik}}{\partial \ln V} \quad (3)$$

$$c_{ik} = \left( \frac{\hbar \omega_{ik}}{k_B T} \right)^2 \frac{\exp\{\hbar \omega_{ik}/(k_B T)\}}{[\exp\{\hbar \omega_{ik}/(k_B T)\} - 1]^2} \quad (4)$$

where  $V$  is the molar volume,  $\omega_{ik}$  is the harmonic frequency of the  $ik$ -th phonon, and  $k_B$  is the Boltzmann constant. A premise is that  $\gamma_{ik}$  is nearly constant across a range of volume.

The mode heat capacity is related to the unit-cell isochoric heat capacity ( $\tilde{C}_V$ ) and molar isochoric heat capacity ( $C_V$ ) by

$$\tilde{C}_V = \frac{1}{K} \sum_i \sum_{\mathbf{k}} c_{ik} \quad (5)$$

$$C_V = \frac{R}{N_{\text{mol}}} \tilde{C}_V \quad (6)$$

where  $R$  is the gas constant and  $N_{\text{mol}}$  is the number of molecules in a unit cell (four in  $\text{CO}_2$ -I).

The structures (including  $V$ ) and phonon frequencies ( $\omega_{ik}$ ) of an infinite, three-dimensional crystal of  $\text{CO}_2$ -I were obtained as a function of pressure ( $P$ ) at 0 K using the embedded-fragment MP2 method<sup>15</sup> with the aug-cc-pVDZ basis set from our previous studies.<sup>20,21</sup> Additionally, the structures were determined by MP2 with the aug-cc-pVTZ basis set and a counterpoise correction<sup>22</sup> for BSSE in this study (the prefix

"cp-" denotes the counterpoise correction). The details of the electronic structure calculations can be found in refs 20 and 21, and the algorithm of the normal-mode analysis is in Appendix A of ref 23. It may be emphasized that MP2 is a member of systematically converging *ab initio* methods and can describe covalent, ionic, hydrogen-bond, and dispersion interactions on an equal footing. The embedded-fragment method<sup>16,24</sup> divides a molecular crystal into overlapping dimers of constituent molecules that are embedded in the self-consistently determined point charges emulating the crystalline electrostatic environment.<sup>15</sup> Since this method does not rely on the periodic boundary conditions, phonon frequencies throughout the Brillouin zone are obtained without any computational cost penalty.

The isothermal bulk modulus at zero pressure ( $B_0$ ) was obtained by linear-least-squares fitting of the calculated equation of state ( $P$ - $V$  curve) to the third-order Birch–Murnaghan equation:

$$P = \frac{3B_0}{2} \left\{ \left( \frac{V_0}{V} \right)^{7/3} - \left( \frac{V_0}{V} \right)^{5/3} \right\} \times \left[ 1 + \frac{3}{4} (B'_0 - 4) \left\{ \left( \frac{V_0}{V} \right)^{2/3} - 1 \right\} \right] \quad (7)$$

where  $B'_0$  is the pressure derivative of  $B$  at zero pressure.

The values of  $\gamma_{ik}$  were obtained for each dispersion branch on a  $10 \times 10 \times 10$  grid of wave vectors in the reciprocal unit cell within the following approximation

$$\gamma_{ik} = -\frac{\ln \omega_{ik}^{(10\text{GPa})} - \ln \omega_{ik}^{(0\text{GPa})}}{\ln V^{(10\text{GPa})} - \ln V^{(0\text{GPa})}} \quad (8)$$

where the superscripts should be self-explanatory. Using  $\omega_{ik}$ ,  $c_{ik}$  and  $C_V$  were also calculated with eqs 4 and 5, which led to  $\alpha_L$ .

## 3. RESULTS AND DISCUSSION

**3.1. Heat Capacity.** Figure 1 plots the observed values<sup>25</sup> of  $C_p$  and observed<sup>4</sup> and calculated values of  $C_V$  as a function of temperature. The differences between observed  $C_p$  and  $C_V$  are negligible until 80 K, where  $C_V$  slows its increase as compared with  $C_p$ . The observed values of  $C_V$  were, in fact, calculated from the directly measured values of  $C_p$  by Manzhelii et al.<sup>4</sup> using the relation<sup>1</sup>  $C_p - C_V = 9\alpha_L^2 BVT$ . The MP2-calculated values of  $C_V$  are in good agreement with the observed values at low temperatures ( $T < 15$  K) and are too low by 10% near 100 K. The underestimation is typical of such calculations and is largely ascribed to the neglect of anharmonicity. The curve of the MP2-calculated  $C_V$  appears more parallel to that of the observed  $C_V$  (as opposed to  $C_p$ ).

At very low temperatures, both observed and calculated  $C_V$  display Debye's  $T^3$  behavior, as shown in the inset. This is unlike water ice (ice Ih), in which weak hydrogen-bond vibrations serve as a heat reservoir at low temperatures and cause a deviation from the  $T^3$  behavior.<sup>26</sup> The Debye temperature of the MP2 result at 5 K is 154 K, which is in good agreement with the observed value of  $152 \pm 1.5$  K.<sup>4</sup>

**3.2. Bulk Modulus.** The calculated and experimental<sup>4,5,11,13,14,27–32</sup> values of  $B_0$  are compiled in Table 1. These values are scattered from 2.9 to 21.9 GPa, depending on the temperature and method of measurement or calculation. Although the high-end value of 21.9 GPa may be an outlier, the rest are rather evenly divided into a group centered around

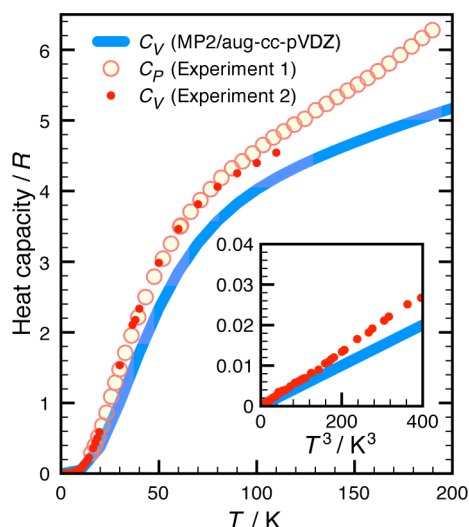


**Figure 1.** Calculated and observed isobaric and isochoric heat capacities ( $C_P$  and  $C_V$ ) of  $\text{CO}_2$ -I as a function of temperature ( $T$ ). Experiments 1 and 2 are due to Giauque and Egan<sup>25</sup> and to Manzhelii et al.,<sup>4</sup> respectively. The inset plots  $C_V$  as a function of  $T^3$  at low temperatures.

**Table 1.** Molar Volume ( $V_0$ ), Bulk Modulus ( $B_0$ ), and Its Pressure Derivative ( $B'_0$ ) of  $\text{CO}_2$ -I at Zero Pressure

method	$V_0$ ( $\text{cm}^3 \text{mol}^{-1}$ )	$B_0$ (GPa)	$B'_0$
MP2/aug-cc-pVDZ (this work)	23.7	16.1	6.9
cp-MP2/aug-cc-pVTZ (this work)	24.5	12.1	7.7
DFT <sup>33 a</sup>	22.2	16.6	
DFT <sup>34 b</sup>	31.9	3.2	8.1
DFT <sup>35 c</sup>	27.5	9.4	5.5
experiment (190 K) <sup>27</sup>		4.8	
experiment (190 K) <sup>27 d</sup>		3.9	
experiment (77 K) <sup>28 d</sup>		7.9	
experiment (145 K) <sup>28 d</sup>		4.9	
experiment (185 K) <sup>28 d</sup>		4.2	
experiment (13 K) <sup>4 e</sup>	25.9	8.0	
experiment (0 K) <sup>5</sup>	25.8	7.6	
experiment (fit 1; $296 \pm 2$ K) <sup>29 f</sup>	31.4	2.9	7.8
experiment (fit 2; $296 \pm 2$ K) <sup>29 f</sup>	26.6	21.9	4.4
experiment (300 K, 0.6 GPa) <sup>30</sup>		9.5	
experiment (300 K) <sup>31</sup>	25.1	6.2	6.1
experiment (0 K) <sup>32</sup>		3.5	7.8
fit to experiment (0 K) <sup>11</sup>	25.8	10.4	6.8
fit to experiment (0 K) <sup>13,14</sup>	25.8	9.0	

<sup>a</sup>Local-density approximation. <sup>b</sup>Generalized-gradient approximation. <sup>c</sup>Dispersion corrected. <sup>d</sup>These values were obtained by linear-least-squares fitting by Liu<sup>29</sup> of the  $P$ – $V$  curves reported in the respective papers. <sup>e</sup>The value of  $B_0$  is the reciprocal of the compressibility at 0 K, whose value, in turn, was calculated from the observed velocities of ultrasonic waves as well as  $V_0$ ,  $C_V$ , and  $\alpha_L$ .<sup>4</sup> <sup>f</sup>Fit 2 was dismissed by Liu<sup>29</sup> for a greater variance than “fit 1”, though they both interpolate the experimental data well.

4 GPa and another about 8 GPa; there is not even an experimental consensus on the correct value of  $B_0$ . Many of the experimental values are obtained by fitting an empirical equation of state to the observed  $P$ – $V$  curve. They are sensitive to  $V_0$ , and its slight variation can cause an order-of-magnitude change in  $B_0$  (see, e.g., fits 1 and 2 of Liu<sup>29</sup> in Table 1). Perhaps the most reliable value is 8.0 GPa of Manzhelii et al.,<sup>4</sup> as it is determined from the measured velocities of ultrasonic waves at

a low temperature without fitting. It is also close to the low-temperature values reported by Stevenson<sup>28</sup> (7.9 GPa) and by Krupskii et al.<sup>5</sup> (7.6 GPa) as well as to those determined by a global fitting of an equation of state to a large body of experimental data (the last two rows of the table).<sup>11,13,14</sup>

The MP2/aug-cc-pVDZ value of 16.1 GPa is twice as great as these experimental values. Figure 2 illustrates the source of this

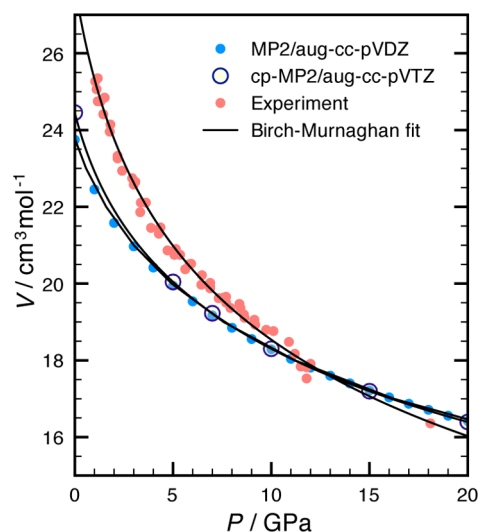


**Figure 2.** MP2-calculated and observed equations of state of  $\text{CO}_2$ -I (see also refs 20 and 21) and the third-order Birch–Murnaghan equation fits. The experimental data at  $296 \pm 2$  K are taken from Liu.<sup>29</sup> The volume collapse at about 11 GPa is caused by a solid–solid phase transition, and the data above that pressure correspond to phase III.<sup>21</sup>

large error. The value of  $B_0$  is proportional to the reciprocal of the slope of the  $P$ – $V$  curve at zero pressure. MP2 predicts a harder, more compact  $\text{CO}_2$ -I than experiment at low pressures, while approaching experimental results under higher pressures.<sup>20</sup> This clearly leads to a greatly amplified difference in the slope,  $\partial P/\partial V$ , at zero pressure between theory and experiment.

The plot of the third-order Birch–Murnaghan equation with the values of  $B_0$  and  $B'_0$  in Table 1 falls on the MP2 values exactly, and in this case, the fitting is not responsible for the error; the overestimation of dispersion interactions by MP2/aug-cc-pVDZ is.<sup>20</sup> It is more severe at lower pressures, where the interactions are weak, and it improves at higher pressures, where the exchange repulsion begins to dominate. The basis set's smallness and BSSE, which can be substantial for dispersion interactions, are implicated in this error.

The cp-MP2/aug-cc-pVTZ calculation indeed predicts a softer  $\text{CO}_2$ -I at low pressures and thus a much smaller value of  $B_0 = 12.1$  GPa. It is closer to the experimental values (8.0 GPa) but still falls short of reaching them. A computational treatment as complex as coupled-cluster singles and doubles with noniterative triples [CCSD(T)] in the complete-basis-set (CBS) limit<sup>36</sup> may be necessary to reproduce  $B_0$  quantitatively. Note that the differences in the absolute values of  $V$  between theory and experiment are largely due to the thermal expansion itself because the experiment was conducted at  $T = 296 \pm 2$  K, while the calculations are at  $T = 0$  K.

Density-functional-theory (DFT) calculations with a local-density approximation<sup>33</sup> and with a generalized-gradient approximation<sup>34</sup> give vastly different predictions for  $V_0$  and  $B_0$ , neither of which seems accurate. When a correction for

dispersion interactions is added,<sup>35</sup> a reasonable value of  $B_0$  is obtained.

In short, it seems exceedingly difficult to determine  $B_0$  accurately either computationally or experimentally.

**3.3. Grüneisen Parameter.** Figure 3 plots  $\ln \omega_{ik}$  as a function of  $\ln V$ . The near linearity of each plot attests to the

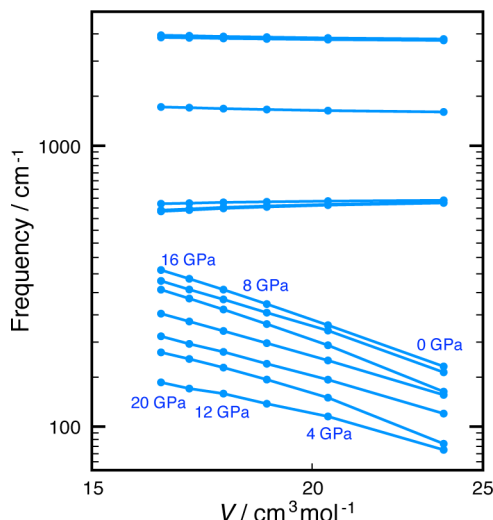


**Figure 3.** A log–log plot of the MP2/aug-cc-pVDZ frequencies of the zone-center phonons of CO<sub>2</sub>-I as a function of volume ( $V$ ).

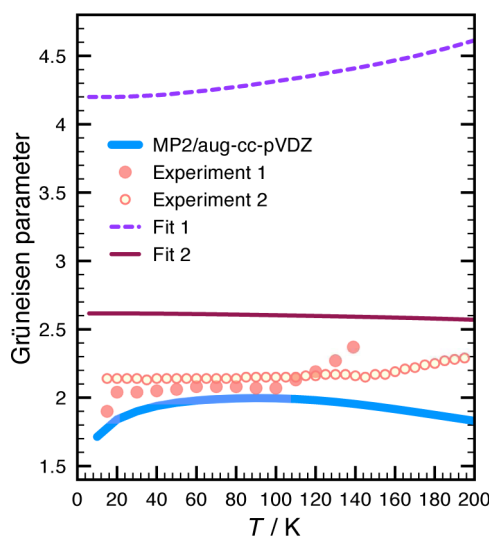
soundness of the premise in Grüneisen's treatment of thermal expansion, that is, the constancy of  $\gamma_{ik}$  with volume. It also justifies our simple way of computing them using the MP2-calculated frequencies at 0 and 10 GPa.

Table 2 compares the calculated and observed<sup>11,13,14,37–39</sup> values of  $\gamma_{ik}$  of the zone-center phonons (except for  $\gamma_{ik}$ 's of acoustic modes, which are obtained at the Z and R points of the Brillouin zone). The MP2 values for the Raman-active ( $E_g$ ,  $F_{g-}$ , and  $F_{g+}$ ) and infrared-active ( $F_{u-}$  and  $F_{u+}$ ) librational modes are in accurate agreement with the most recent experimental estimates.<sup>11</sup> It also reproduces the correct order of the Raman-active librational modes observed by three independent groups.<sup>11,38,39</sup> The agreement inspires confidence in MP2-calculated  $\gamma_{ik}$  for acoustic modes also, which cannot be measured by infrared or Raman spectroscopy.

The table illustrates the significance of the low-frequency (acoustic, pseudotranslational, and librational) modes, which have much greater  $\gamma_{ik}$  and  $c_{ik}$  than the phonons with frequencies

above 500 cm<sup>−1</sup>. The latter have near-zero  $\gamma_{ik}$  and small weight ( $c_{ik}$ ) and thus a negligible contribution in  $\gamma$ . The values of  $\gamma_{ik}$  of the bending modes ( $\nu_2$ ) are negative.<sup>38</sup> We have discussed its effect on the pressure detuning of Fermi resonance in CO<sub>2</sub>-I.<sup>20</sup> All other modes have positive values of  $\gamma_{ik}$ .

Figure 4 plots MP2-calculated and observed<sup>4,5</sup>  $\gamma$  as a function of temperature. They are in good agreement with each other.



**Figure 4.** Grüneisen parameter ( $\gamma$ ) of CO<sub>2</sub>-I as a function of temperature ( $T$ ). Experimental data 1 and 2 are taken from Manzheli et al.<sup>4</sup> and Krupskii et al.,<sup>5</sup> respectively. Fits 1 and 2 are obtained by Giordano et al.<sup>11</sup> and by Trusler,<sup>13,14</sup> respectively, by fitting an empirical equation of motion to experimental data.

MP2 also captures the rise in  $\gamma$  at  $T < 20$  K seen in one of the experimental data sets. On the other hand, MP2 does not reproduce the sudden increase in  $\gamma$  at  $T \approx 100$  K, where MP2-calculated  $\gamma$  begins to decrease slightly. This is consistent with Manzheli's attribution of this to orientational defects, which do not exist in our calculation.

Also plotted in this figure are  $\gamma = \gamma_D(V/V_0)^q$  obtained by fitting an equation of state to experimental thermodynamic and spectroscopic data;<sup>11,13,14</sup> in this plot,  $(V/V_0)$  as a function of temperature is adopted from experiment<sup>5</sup> and only the values of  $\gamma_D$  and  $q$  are taken from these global fitting studies.<sup>11,13,14</sup> The  $\gamma_D$  value of 4.2 adopted by Giordano et al.<sup>11</sup> is more than twice as great as the MP2  $\gamma$  values (ca. 2.0). Furthermore, the former increases nearly linearly with  $V$  because of  $q = 1.1$ , which may

**Table 2.** Mode Grüneisen Parameters ( $\gamma_{ik}$ ) of Phonons in CO<sub>2</sub>-I<sup>a</sup>

mode	exp. <sup>37</sup>	exp. <sup>38</sup>	exp. <sup>39</sup>	exp. <sup>11</sup>	exp. <sup>13,14</sup>	MP2/aug-cc-pVDZ
acoustic (Z)						1.81
acoustic (R)						2.10
$E_g$ ( $\Gamma$ )	$2.3 \pm 0.2$	$1.95 \pm 0.05$	1.8	$1.69 \pm 0.02$		1.60
$F_{g-}$ ( $\Gamma$ )	$2.3 \pm 0.2$	$2.11 \pm 0.06$	1.91	$1.75 \pm 0.01$		1.75
$F_{g+}$ ( $\Gamma$ )	$2.2 \pm 0.2$	$2.22 \pm 0.05$	1.94	$1.82 \pm 0.01$		2.20
$F_{u-}$ ( $\Gamma$ )				$2.1 \pm 0.2$		2.22
$F_{u+}$ ( $\Gamma$ )				$2.1 \pm 0.2$		2.10
$\nu_1$ ( $\Gamma$ ) <sup>b</sup>					0.0633	0.092
$\nu_2$ ( $\Gamma$ ) <sup>c</sup>					−0.0521	−0.111
$\nu_3$ ( $\Gamma$ ) <sup>d</sup>					0.0515	0.067

<sup>a</sup>The symbols in parentheses denote special points in the Brillouin zone. <sup>b</sup>Average of four symmetric stretching modes. <sup>c</sup>Average of eight bending modes. <sup>d</sup>Average of four antisymmetric stretching modes.



be partly responsible for reproducing the rise in  $\gamma$  at 100 K. Since the measured values of  $\gamma_{ik}$  for the zone-center librational modes are only ca. 2 or less, Giordano et al. speculated that acoustic modes dominate in  $\gamma$  and their  $\gamma_{ik}$  values were also much greater. Our MP2 calculation suggests otherwise: The values of  $\gamma_{ik}$  for acoustic modes are no greater than those of the librational modes (see Table 2). They should indeed be smaller on average, as suggested by the increase in  $\gamma$  below  $T \approx 20$  K observed in both the experimental<sup>4</sup> and MP2 data. The  $\gamma$  curve of Trusler<sup>13,14</sup> is more in line with the MP2 result. It is nearly constant at 2.6, decreasing slightly with temperature.

Figure 5 displays the phonon dispersion curves of CO<sub>2</sub>-I at 0 and 10 GPa in the low-frequency region along the [111]

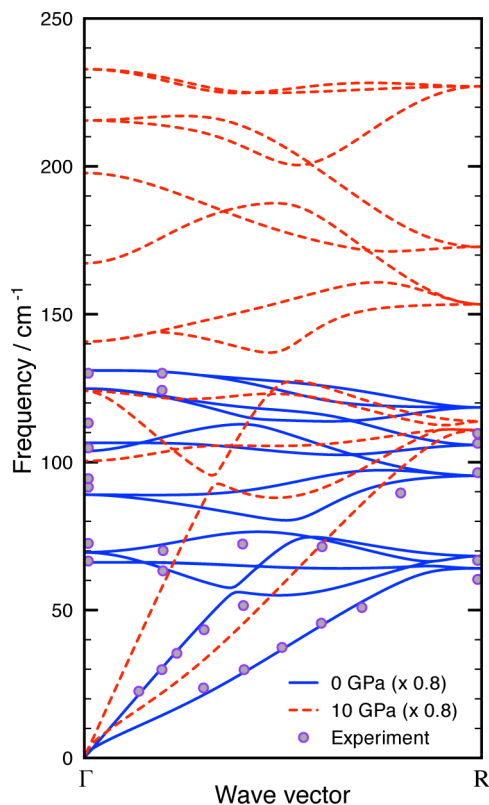


**Figure 5.** MP2/aug-cc-pVDZ phonon dispersions in CO<sub>2</sub>-I at 0 and 10 GPa. The calculated frequencies are scaled by 0.8 just to make the comparison with the experimental data from Powell et al.<sup>40</sup> easier.

direction. Superimposed are the experimental data obtained by Powell et al.<sup>40</sup> using inelastic neutron scattering. The calculated frequencies systematically overestimate the observed frequencies for the same reason that MP2 overestimates the cohesive forces at 0 GPa and underestimates the volume. Nevertheless, the general shape of the dispersion curves is reproduced, and when the calculated frequencies are scaled by 0.8, they agree with the observed frequencies quantitatively. The comparison between the 0 and 10 GPa curves testifies that the frequency increase upon pressure loading is slightly greater in librational modes than in acoustic modes, which translates to smaller  $\gamma_{ik}$  for acoustic modes.

**3.4. Thermal Expansion Coefficient and Thermal Pressure Coefficient.** Figure 6 compares the MP2-calculated linear thermal expansion coefficient ( $\alpha_L$ ) with experiments.<sup>4,41</sup> The MP2/aug-cc-pVDZ curve is twice as small as the experimental results, and given the reasonably accurate

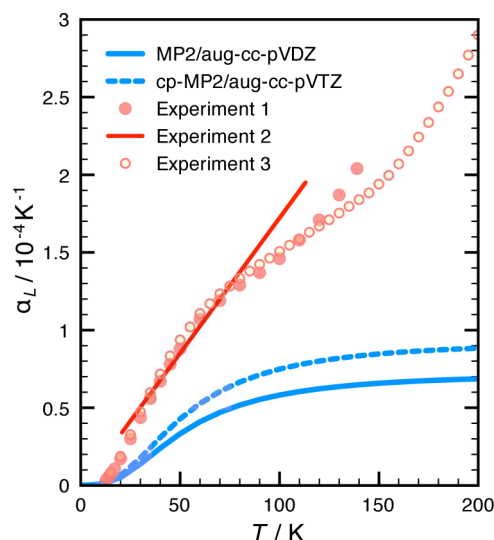


**Figure 6.** Linear thermal expansion coefficient ( $\alpha_L$ ) of CO<sub>2</sub>-I as a function of temperature ( $T$ ). Experimental data 1–3 are taken from Manzhelii et al.,<sup>4</sup> Keesom and Köhler,<sup>41</sup> and Krupskii et al.,<sup>5</sup> respectively.

predicted values of  $C_V$ ,  $\gamma$ , and  $V_0$ , this is nearly entirely ascribed to the error in  $B_0$ . When the cp-MP2/aug-cc-pVTZ values of  $B_0 = 12.1$  GPa and  $V_0 = 24.5$  cm<sup>3</sup> mol<sup>−1</sup> are used instead (with all the other factors unchanged), the calculated results are improved somewhat. The use of the experimental value of  $B_0 = 8.0$  GPa erases nearly all of the errors. Again, therefore, the discrepancy between theory and experiment is traced to the difficulty in predicting  $B_0$ .

The thermal pressure coefficient denoted by  $\beta$  in this article and defined by

$$\beta \equiv \left( \frac{\partial P}{\partial T} \right)_V = B_0 \alpha_V \quad (9)$$

does not involve  $B_0$ ; the factor  $B_0$  in eq 9 cancels the same in  $\alpha_V$ , rendering  $\beta$  independent of it. This quantity has been directly measurable for liquids<sup>17,18</sup> and rare gas solids.<sup>1</sup> The MP2 and experimental values of  $\beta$  may be obtained by multiplying the respective values of  $\alpha_L$  by  $3B_0$ . Since the MP2 values of  $B_0$  and  $\alpha_L$  are too large and too small, respectively, both by a factor of 2, the MP2 and experimental values of  $\beta$  agree with each other well up to 100 K (not shown).

## 4. CONCLUSION

MP2/aug-cc-pVDZ can reproduce from the first-principles the observed values of  $C_V$ ,  $\gamma$ , and  $V_0$  of CO<sub>2</sub>-I—the factors entering the expression of  $\alpha_L$ —sufficiently accurately (within 10% or so). However, it cannot predict the value of  $B_0$  with the same accuracy, resulting in a large systematic error in  $\alpha_L$ . A small deviation in the  $P$ – $V$  curve between theory and experiment is greatly amplified in  $B_0$ , which is the derivative of the  $P$ – $V$  curve at zero pressure. This is traced to the tendency of MP2/aug-cc-pVDZ to overestimate dispersion interactions, which are mainly responsible for the cohesive forces in CO<sub>2</sub>-I, along with the quadrupole–quadrupole interactions. The use of a counterpoise correction for BSSE and the aug-cc-pVTZ basis set improves the value of  $B_0$  by 25% but falls short of erasing the error in  $\alpha_L$ ; it may be necessary to employ CCSD(T)/CBS to determine  $B_0$  quantitatively. Even the experimental values of  $B_0$  are not mutually consistent, especially when they are

determined from observed  $P$ – $V$  curves by fitting. The thermal pressure coefficient  $\beta$ , which is directly measurable and does not depend on  $B_0$ , is reproduced reasonably accurately by MP2 up to 100 K.

## AUTHOR INFORMATION

### Corresponding Author

\*E-mail: sohirata@illinois.edu.

### Funding

This material is based on work supported by the National Science Foundation under CHE-1361586.

### Notes

The authors declare no competing financial interest.

## ACKNOWLEDGMENTS

S.H. is a Camille Dreyfus Teacher-Scholar and a Scialog Fellow of the Research Corporation for Science Advancement.

## REFERENCES

- (1) Wallace, D. C. *Thermodynamics of Crystals*; Wiley: New York, 1972.
- (2) Hemley, R. J. *Annu. Rev. Phys. Chem.* **2000**, *51*, 763.
- (3) Maass, O.; Barnes, W. H. *Proc. R. Soc. A* **1926**, *111*, 224.
- (4) Manzhelii, V. G.; Tolkachev, A. M.; Bagatskii, M. I.; Voitovich, E. I. *Phys. Status Solidi B* **1971**, *44*, 39.
- (5) Krupskii, I. N.; Prokhvatilov, A. I.; Érenburg, A. I.; Baryl'nik, A. S. *Fiz. Nizk. Temp.* **1982**, *8*, 533.
- (6) Suzuki, M.; Schnepf, O. *J. Chem. Phys.* **1971**, *55*, 5349.
- (7) Gibbons, T. G.; Klein, M. L. *J. Chem. Phys.* **1974**, *60*, 112.
- (8) Kobashi, K.; Kihara, T. *J. Chem. Phys.* **1980**, *72*, 3216.
- (9) LeSar, R.; Gordon, R. G. *J. Chem. Phys.* **1983**, *78*, 4991.
- (10) Etters, R. D.; Kuchta, B. J. *J. Chem. Phys.* **1989**, *90*, 4537.
- (11) Giordano, V. M.; Datchi, F.; Gorelli, F. A.; Bini, R. *J. Chem. Phys.* **2010**, *133*, 144501.
- (12) Jäger, A.; Span, R. *J. Chem. Eng. Data* **2012**, *57*, 590.
- (13) Trusler, J. P. M. *J. Phys. Chem. Ref. Data* **2011**, *40*, 043105.
- (14) Trusler, J. P. M. *J. Phys. Chem. Ref. Data* **2012**, *41*, 039901.
- (15) Hirata, S. *J. Chem. Phys.* **2008**, *129*, 204104.
- (16) Hirata, S.; Gilliard, K.; He, X.; Li, J.; Sode, O. *Acc. Chem. Res.* **2014**, *47*, 2721.
- (17) Westwater, W.; Frantz, H. W.; Hildebrand, J. H. *Phys. Rev.* **1928**, *31*, 135.
- (18) Hildebrand, J. H. *Phys. Rev.* **1929**, *34*, 649.
- (19) Kittel, C. *Introduction to Solid State Physics*; Wiley: New York, 1966.
- (20) Sode, O.; Keçeli, M.; Yagi, K.; Hirata, S. *J. Chem. Phys.* **2013**, *138*, 074501.
- (21) Li, J.; Sode, O.; Voth, G. A.; Hirata, S. *Nat. Commun.* **2013**, *4*, 2647.
- (22) Kamiya, M.; Hirata, S.; Valiev, M. *J. Chem. Phys.* **2008**, *128*, 074103.
- (23) Sode, O.; Hirata, S. *Phys. Chem. Chem. Phys.* **2012**, *14*, 7765.
- (24) Gordon, M. S.; Fedorov, D. G.; Pruitt, S. R.; Slipchenko, L. V. *Chem. Rev.* **2012**, *112*, 632.
- (25) Giaque, W. F.; Egan, C. J. *J. Chem. Phys.* **1937**, *5*, 45.
- (26) He, X.; Sode, O.; Xantheas, S. S.; Hirata, S. *J. Chem. Phys.* **2012**, *137*, 204505.
- (27) Bridgman, P. W. *Proc. Am. Acad. Arts Sci.* **1938**, *27*, 207.
- (28) Stevenson, R. J. *J. Chem. Phys.* **1957**, *27*, 673.
- (29) Liu, L. G. *Earth Planet. Sci. Lett.* **1984**, *71*, 104.
- (30) Shimizu, H.; Kitagawa, T.; Sasaki, S. *Phys. Rev. B* **1993**, *47*, 11567.
- (31) Yoo, C. S.; Kohlmann, H.; Cynn, H.; Nicol, M. F.; Iota, V.; LeBihan, T. *Phys. Rev. B* **2002**, *65*, 104103.
- (32) Zhang, J. S.; Shieh, S. R.; Bass, J. D.; Dera, P.; Prakapenka, V. *Appl. Phys. Lett.* **2014**, *104*, 141901.
- (33) Garcia, L.; Marqués, M.; Beltrán, A.; Martín Pendás, A.; Recio, J. M. *J. Phys.: Condens. Matter* **2004**, *16*, S1263.
- (34) Bonev, S. A.; Gygi, F.; Ogitsu, T.; Galli, G. *Phys. Rev. Lett.* **2003**, *91*, 065501.
- (35) Gohr, S.; Grimme, S.; Sohnel, T.; Paulus, B.; Schwerdtfeger, P. *J. Chem. Phys.* **2013**, *139*, 174501.
- (36) Sinnokrot, M. O.; Sherrill, C. D. *J. Phys. Chem. A* **2006**, *110*, 10656.
- (37) Schmidt, J. W.; Daniels, W. B. *J. Chem. Phys.* **1980**, *73*, 4848.
- (38) Hanson, R. C.; Jones, L. H. *J. Chem. Phys.* **1981**, *75*, 1102.
- (39) Olijnyk, H.; Dauber, H.; Jodl, H. J.; Hochheimer, H. D. *J. Chem. Phys.* **1988**, *88*, 4204.
- (40) Powell, B. M.; Dolling, G.; Piseri, L.; Martel, P. *Neutron Inelastic Scattering*; International Atomic Energy Agency: Vienna, Austria, 1972; p 207.
- (41) Keesom, W. H.; Köhler, J. W. L. *Physica* **1934**, *1*, 655.